BAV MAGAZINE
SPECTROSCOPY
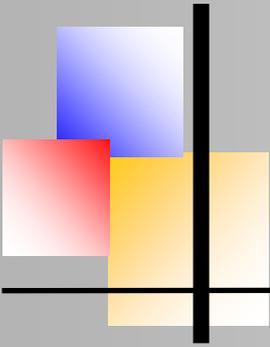

OF THE GERMAN ORGANIZATION
&
WORKING GROUP
VARIABLE STARS BAV

BAV MAGAZINE SPECTROSCOPY

EDITORIAL

From the stars we basically receive only their electromagnetic radiation of different wavelengths, and we "see" essentially only the surface of the radiating bodies. By evaluating the light, we obtain information about:

- the direction of the radiation (positions and movement of the stars)
- the quantity of the radiation (brightness)
- the quality of the radiation (color, spectrum, polarization)

For amateurs, only the narrow band of visible light is easily accessible. In this spectral region, however, both the brightness (photometry) and the spectra of the objects can be examined. Today's amateur astronomy, with its instrumental and computer-assisted equipment, enjoys observation possibilities that were reserved exclusively for professional astronomers until a few years ago.

Thanks to the development of CCD technology, the types of observational perspectives have become much more varied. For example, in the area of variable star observation, there are many new possibilities in addition to already existing approaches.

Professional variable star research employs techniques and observation methods to study the physics and atmospheres of the stars in a holistic manner, considering all aspects and occurrences. Thus, this means that the collected radiation must be understood as a complex storage medium of the physical processes on and in the observed star.

This is appropriate for the intensity of the light, as well as for its spectral composition. The linking of brightness measurements and spectroscopy, a matter of course in professional astronomy, reflects this connection.

Along with brightness changes that occur in variable stars (which can occur quite frequently) variable changes in the state of the stars also can take place and often are revealed in the corresponding spectrum.

Ernst Pollmann
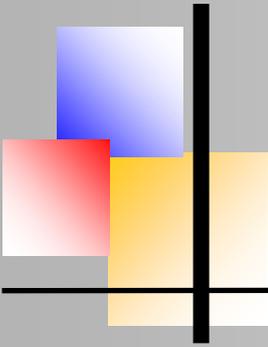
BAV MAGAZINE SPECTROSCOPY

Editorial

Ernst Pollmann, 51375 Leverkusen, Emil-Nolde-Straße 12, ernst-pollmann@t-online.de
Lienhard Pagel, 18311, Klockenhagen Mecklenburger Str. 87, lienhard.pagel@t-online.de
Roland Bücke, 21035 Hamburg, Anna von Gierke Ring 147, rb@buecke.de
The authors are responsible for their contributions.
Coverpicture:
HRDT2 (Astronomy & Astrophysics Royal Observatory of Belgium)

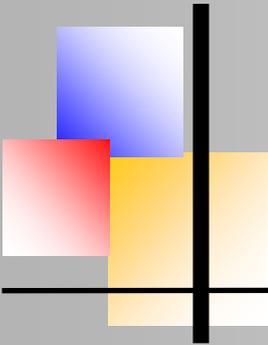**Content**   **Page**

About the properties and problems of Be stars
Michael Winkhaus (CFG observatory Wuppertal, Germany)

1 Introduction
1.1 Emission line stars of spectral type Be

Some hot (blue) stars are surrounded by glowing cool rings of gas, indicated by the appearance of unusual emission lines in their spectra. From the late O to the early A stars about 15% show hydrogen (Balmer) lines in their optical spectra at least temporarily, as well as FeII and MgII lines in emission, in contrast to the normal early-type stars.

The phenomenon observed in many hot stars, that spectral lines appear as bright (emission) lines on the fainter background of the continuum, was found in the first systematic survey of the spectra of over 500 stars by the Italian Angelo Secchi (1818-1878). In 1866, Secchi had inspected the star spectra on the roof of the church of Sant'Ignazio in the middle of the city of Rome using a refractor with an aperture of 24 cm and noticed bright Fraunhofer lines in the spectra of the stars gamma Cas and beta Lyr. Since the first general assembly of the IAU (International Astronomical Union) in 1922, stars of the spectral type "B" with emission lines in their spectra have been referred to as "emission line stars of spectral type B" or simply as Be stars [1]. The "classical" Be stars in the narrower sense are today understood to be the stars of spectral type B on or near the main sequence (i.e. stars of luminosity classes III to V), in whose spectrum emission lines were noticed at least once.

Since about 20% of all stars of luminosity class III to V of spectral type B1 to B5 appear as Be stars [2], this phenomenon must certainly be taken into account with regard to model considerations for stellar evolution. The other early-type stars with these spectral properties (Oe and Ae stars) essentially only differ from the Be stars by a larger or smaller effective temperature [3]. In the Herzsprung-Russel diagram, the Be stars lie on average 0.5 to 1.0 mag above the main sequence. Some Be stars change their relative position to the main sequence over time scales of years due to variability in their brightness [2]. It is also important that some Be stars temporarily do not show any emission lines, so that they have transitioned into the stage of a normal B star in the meantime, but can later show the characteristic Be phenomenon again.

1.2 Properties of Be stars
1.2.1 Emission Lines

The emission lines that appear in stellar spectra generally arise in extended atmospheres or envelopes that are optically thin (i.e., transparent) to the continuous stellar radiation outside the lines. The atoms or ions of this shell are excited by the central star (by the UV radiation it emits) and thus shine in the light of its spectral lines. The (large) envelope therefore radiates much brighter in the spectral lines emitted by it than the (smaller) central star embedded in it.
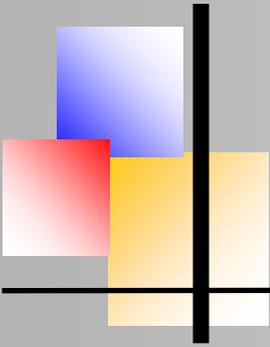
Finally, an example is the sun with its emission lines of the chromosphere and corona, which, however, are not significant compared to the continuum of the photosphere.

The shapes of the emission lines in Be stars are primarily determined by the Doppler effect of the emitting atoms and therefore reflect the movement of the gas in the associated regions (Doppler broadening) and the radial velocities of the overall system (star + envelope) relative to the observer (Doppler shift).

The strongest emission lines in the optical spectra of Be stars are the first Balmer lines (H The long-term analysis of many Be spectra now shows that the V/R asymmetries of typical double-peak profiles usually show the same direction for a few years, but then often turn in the opposite direction and remain in this direction for a few years, until finally another Reversal of the asymmetry in the first observed direction occurs. The period length of consecutive cycles of such V/R variations are i.a. not strictly constant and also vary noticeably with different Be stars. Mean cycle times are between a few years and a few decades [14].

The cyclic variations in the relative double peak intensities are usually associated with corresponding cyclic variations in the radial velocities of the intensity maxima and the central absorption components of the profiles. The brighter emission peak seems to move towards the middle of the line with increasing intensity [10]. Hα, Hβ) of hydrogen and the lines of singly ionized iron (FeII), the higher Balmer lines (H8…H15) rarely show emissions [4]. The photospheric absorption lines (mainly H and HeI) of these stars are usually very much broadened.

1.2.2 High rotation velocities

The significant broadening of the photospheric absorption lines (especially visible for HeI) indicate very high rotation speeds of the stars. One obtains equatorial speeds of up to 450 km/s [5], which corresponds to about 200 times the rotation speed of our sun.

The true equatorial rotation velocities v of the Be stars cannot be measured directly, since the rotation axes of the stars are tilted at an unknown angle to the viewing direction. Only the velocity v sin i projected onto the observation direction can be measured spectroscopically, i.e. the product of true rotation velocities v and the sine of the inclination i, the angle between the orientation of the rotation axis of the star and the line of sight of the observer. At i = 0° you look at the pole of a star, at i = 90° at the equator. It is common to speak of "pole-on" stars for v sin i < 150 km/s (i < 15°), stars with v sin i > 300 km/s (i > 60°) are called "equator -on" stars. The largest known values for v sin i are about 450 km/s for Be stars, so that the true rotation speeds should also be in this order of magnitude. From the observed statistical increase in the abundance
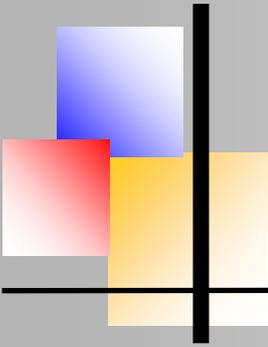
of Be stars with increasing v sin i , Slettebak [6] concluded that Be stars rotate with a fairly u-niform true rotation rate of v = 450-500 km/s and the variation in measured projected rotation rates alone through the statistical distribution of the orientation of the rotation axes comes about.

It is remarkable that this estimation results in approx. 80% of the critical equatorial speed (compensation of centrifugal force and gravitation) for the respective star, so that the Be stars should be clearly flattened. This flattening leads to a decrease in the effective gravitational acceleration geff from the pole to the equator (geff = g–gz). Assuming hydrostatic equilibrium in the stellar atmosphere, the Zeipel theorem (1922) states that the local bolometric radiant flux F at the stellar surface is proportional to the effective gravitational acceleration geff. From this follows immediately $\sigma T_{eff}^4 \sim g_{eff}$, i.e. a decrease in the effective temperature and the brightness with decreasing effective gravitational acceleration. Rotating and therefore flattened stars therefore appear cooler when viewed at high inclination ("equator-on"). This variation of effective temperature with inclination thus directly affects spectral type, such that a "pole-on" star is assigned an earlier spectral type than the same star seen "equator-on" ("gravitational eclipsing").

In addition, significant rotational instabilities can be expected in the area of the stellar equator. According to a suggestion by Struve (1931) and McLaughlin (1961), such rotational instabilities and possibly also selective radiation pressure in the area of the stellar equator can cause layers to detach, which, in the equilibrium of centrifugal and gravitational acceleration, gradually form an at least temporarily stationary envelope or a form a ring of rarefied gas that rotates slower than the stellar photosphere due to conservation of angular momentum. The emission lines excited by the UV radiation throughout the envelope therefore show smaller Doppler shifts than the photospheric absorption lines.

Overall, the result is a model of a rapidly rotating, flattened Be star surrounded by a flat rotating annular or disc-shaped gas shell, which has its greatest extent in the equatorial plane of the star. Typical disk diameters are 5 to 10 star diameters. Therefore, the temperature of the emitting disk gas must be much lower than the temperature of the stellar surface. We can thus speak of a glowing cool gas disk around the Be star.

1.2.3 Be star radiation is polarized
The disk model for the circumstellar envelopes of Be stars is supported by the important finding that the radiation emitted by Be stars exhibits a small but distinct polarization (about 1%) that does not occur in normal spherically symmetric stars without an envelope [1]. The strength of the polarization increases with the projected rotation speed, so that the measured polarization directions presumably directly show the orientations of the rotation axis of the Be stars in the sky.
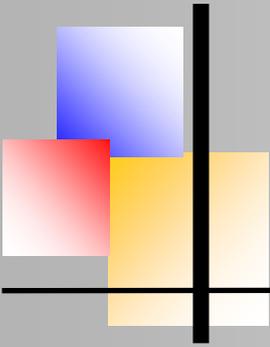
Finally, direct confirmation of the gas ring model of Be stars could be provided by the first precise determination of the dimensions of the circumstellar disks and their flattening using Michelson stellar interferometers. The obtained position angles of the semimajor axis of the obliquely viewed gas ring of γ Cas agreed well with the position angle known from polarization measurements [1].

Statistical investigations on large amounts of Hα measurements ([10] + [11]), as well as observations in other spectral ranges (UV, IR), also speak for an oblate geometry of the Be star envelopes, so that the idea of a strongly oblate envelope today is no longer doubted.

1.2.4 Physical properties of the gas disks

The physical properties of the circumstellar gas rings (shape, dimensions, gas density and its distribution, temperature, state of motion…) are difficult to determine and have not been adequately researched to date. In order to determine them, assumptions about the basic properties of the central star (mass, radius, eff. temperature, equatorial velocity, angle of inclination i) must be made, as well as some assumptions about the gas ring (inner radius, orbital velocity).

Different methods resulted in typical ring radii of 1.5 to about 30 star radii [1], with the size of the gas rings increasing on average with the strength (equivalent width) of the emission lines.

Statements about the typical thickness of the gas rings can be derived from the fact that about 15% of the bright Be stars show shell profiles [7]. Assuming statistically distributed inclinations of the rotation axes against the direction of observation, it can be concluded that the thickness of the gas rings must be related to their expansion by about 0.15, i.e. about 1:7. Thus the thickness of the disk is small compared to the equatorial extent, but in some cases it can still be several stellar radii.

The theoretical disk models, which quantitatively correctly describe the continuous spectra of the gas disk, require characteristic particle densities of the order of $N \approx 10^{12}$ cm^{-3} and electron temperatures of around 10^4 K for the ionized disk gas in the inner regions of the shell [8].

1.3 Models for the formation of circumstellar gas disks

The rotation model proposed by Struve (1931) and further developed by McLaughlin (1961) is based on the assumption that the Be stars rotate at the equator with critical speed and form a gas disk around the star in the equilibrium of centrifugal and gravitational acceleration. However, since the measured values of v sin i are always below the critical velocity, the stability of the temporal development of these gas disks cannot be explained with this idea alone.
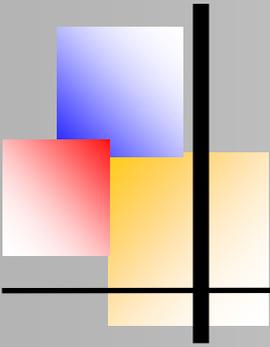
That is why other models are being discussed in Be star research today, which are briefly outlined below. All models are of course constructed using numerous simplifications and can therefore only describe partial aspects of the Be phenomenon due to the complexity of the overall context.

1.3.1 Binary Star Model

The binary star hypothesis [9] assumes that Be stars are close binary stars with mass exchange and that the companion star transfers mass to the B star, so that an accretion disk can form around it. So far, however, Be stars have only been identified as binary stars in isolated cases (e.g. HR2142 [10]. For most Be stars, there are no indications that they are spectroscopic binary stars with sufficiently short orbital periods. It is therefore doubtful that this hypothesis is true for all Be stars.

1.3.2 Pulsation model

Comparable to the pulsating stars of the type β Cep, this model tries to explain the mass loss and the structure of the circumstellar envelope through instabilities of the outer layers of the star, which are often noticeable in non-radial pulsations [11]. However, the connection between non-radial pulsations and the formation of the envelope is unclear, as is possible interaction with the stellar wind.

1.3.3. Stellar wind model

In the stellar wind model, the radiation pressure (assisted by the high rotation and the resulting reduced gravitational acceleration) blows away the outer layers of the photosphere. The material blown away from the star then builds up the circumstellar envelope. A difficulty of this model is that a stellar wind driven by radiation pressure should have the greatest strength in the polar region due to the higher effective temperature. The greatest expansion of the disks is observed in the equatorial direction. It is therefore very unlikely that a high orbital angular momentum circumstellar shell is formed in the equatorial region by material from the polar region with its relatively low angular momentum.

A new attempt to explain the Be phenomenon sees the formation of the rotating circumstellar gas disk as a result of the accumulation of stellar wind material that does not reach the escape velocity or that is slowed down by a shock wave when it hits slower-flowing gas. If such material accumulates in large quantities in the gravitational field of the star, "outsourcing" to an outer disk seems possible [12]. However, this model proposed by Bjorkman and Cassinelli predicts relatively high radial velocities in the disk, which are not observed. Hanuschik et al. (1993) alternatively suggest that because of the small effective gravitational acceleration geff at the stellar surface, a small radial force might be sufficient to form a disk. The interaction of stellar wind andf a
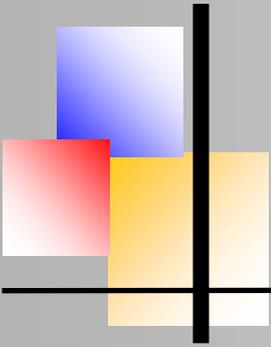
and magnetic activity could support disk formation. So far, the interaction of the mechanisms just described and the significance of a possible interaction between the rapidly rotating star and the extended envelope that is present at least temporarily, as well as the stellar wind, have not been clarified. Overall, the causes of the formation of such gas rings around Be stars are still controversial and not yet understood.

1.4 Basic shape of the Hα spectra

Despite the diverse structures in the emission spectra of the Be stars, it is possible to classify most of the observed line profiles into a unified scheme. The individual shape of the profiles seems to depend on three parameters:

- Inclination (inclination angle i) and the resulting projection effects
- Optical depth τ and radiative transfer effects
- Kinematics and the resulting Doppler interpretation

However, the emission lines are also broadened by thermal movements, which are of the order of approx. 20 km/s for these cool disks [10]. With observed kinematic (Kepler) velocities in the range of 200-500 km/s, this component can be neglected here.

1.4.1 Inclination and optical depth

The origin of the special forms of the observed Hα spectral lines can be understood using the schematic model of a rapidly rotating (hot) Be star with a differentially rotating flat equatorial gas disk. The following figure, which is then explained, is used for this purpose:
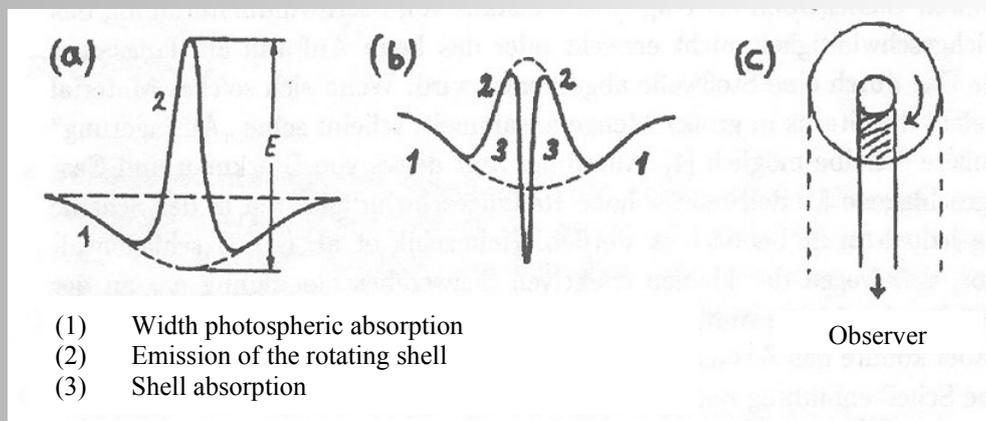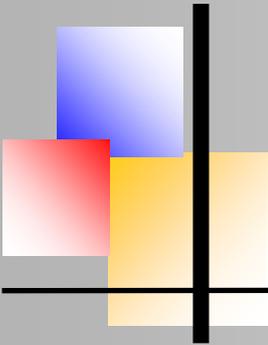

(1)	Width photospheric absorption
(2)	Emission of the rotating shell
(3)	Shell absorption

Observer

Fig. 1: The three typical linie profiles of Be stars (from Voigt, Abriss der Astronomie, P. 172)

About the properties and problems of Be stars

• **1st component:** *from the photosphere of the central star*
A broad absorption line due to the high rate of rotation of the stellar surface

• **2nd component:** *from the interior of the circumstellar gas ring*
Because of the star's strong UV radiation, there are many excited states in this inner region, which then emit radiation. Because of the differential rotation v (shell inner) $< v$ (star), a somewhat narrower emission line follows (see Fig. 1a).

• **3rd component:** *from the outer region of the circumstellar gas ring*
There are considerably fewer excited states. Rather, the atoms in the outer shell absorb the line radiation emitted by the inner areas in a narrow tube which, seen from the observer, just covers the star disk (see Fig. 1c). The orbital motion of this gas is anyway slower and essentially perpendicular to the line of sight because v (shell out) $< v$ (shell inner), so that no noticeable rotational broadening occurs. This then results in a narrow envelope absorption line (see Fig. 1b). However, this third component is only important for long light paths through the shell, i.e. for high inclination angles (i $> 70°$) (see Fig. 2).

The superimposition of these three components results in the typical Be star line profiles (see Fig. 2 below), with the extent of the envelope absorption being essentially determined by the length of the light path through the envelope. The length of the light path naturally depends on the angle of inclination i, as can be seen in Fig. 2.
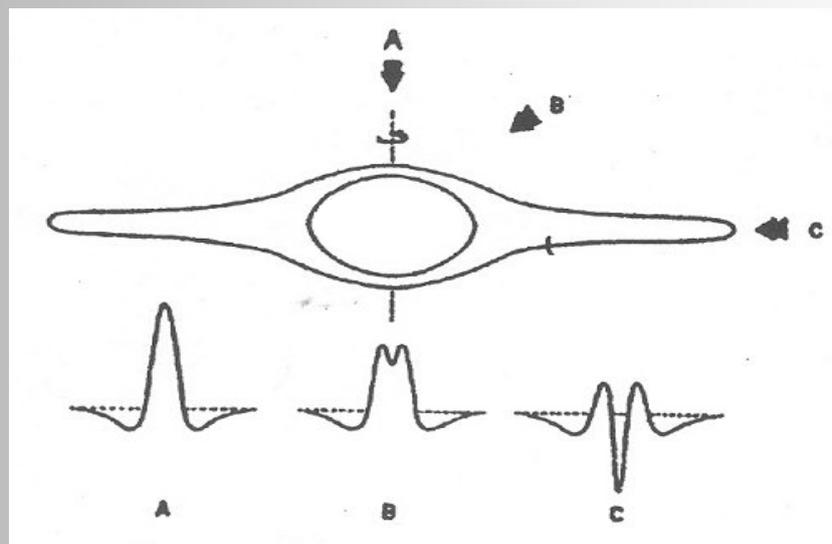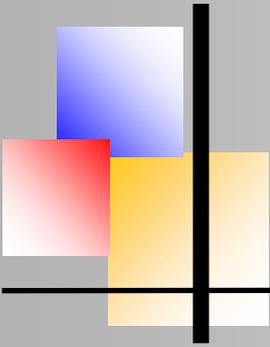

Fig. 2: Rotation modell of O. Struve; Emission line profiles at inklination $i = 0°$ (A), $i = 45°$ (B) and $i = 90°$ (C); (from: Slettebak, The Be-Stars [1979], S. 547)

But consider that the second parameter, in addition to the length of the light path, is also the optical thickness of the shell, which depends on the density and the distribution of the gas in the circumstellar disk. And especially with the Hα spectra, the optical thickness plays a central role. If one transfers interstellar element abundances to the chemical composition of the circumstellar Be gas disks, then a hydrogen content of 90% can be expected. The Hα lines are therefore optically thick and are essentially shaped by the effects of radiative transfer.

An important contribution to the shape of optically thick line profiles is the broadening caused by incoherent scattering [13]. For optically thick lines, deep layers in the disk become visible in the wings of the envelope absorption, not in the center of the line. As the source function increases with depth, the resulting line profile appears as a double peak and is quite a bit broader than in the thermal case [10].

At high inclination (i > 80°), shell absorption of photospheric light becomes important, causing a deep central depression below the stellar continuum. The profile named C in Fig.2 is therefore referred to as the "Shell" profile. Phenomenologically, the associated "shell" stars form a special group of Be stars: their "shell absorptions" cut very deeply and sharply into the continuum. However, the difference between shell stars and normal Be stars is not quantitative, but only arises from the different extents and densities of the regions of the shells that are effective in the direction of observation.

1.4.2 Kinematics

For a basic understanding of the observed line profiles due to kinematic effects, we first restrict ourselves to disks with an axisymmetric velocity field and a density distribution that behaves like a Kepler disk in hydrostatic equilibrium. In a Kepler disk, the shell particles move on approximately circular paths with orbital velocities close to Kepler's value ($v_K(r) \propto r^{-0.5}$), so that we assume a differential rotation in the disk.

Such a disk naturally provides symmetrical line profiles. It is to be expected that all lines are shaped by the influence of kinematic Doppler broadening. If you look through the shell (ie at $i \neq 0$), the kinematic profile appears double-peaked and broadened, as the two following illustrations make clear.

The radiation of the line appears to be shifted to smaller or larger wavelengths as a result of the disk rotation, depending on whether the emitting areas of the disk are moving towards or away from the observer. The innermost areas of the disk rotate the fastest, causing the largest line shifts, but because of their small volume, they contribute little to the line profile. Gas moving across the line of sight does not produce line shift Fig. 3).
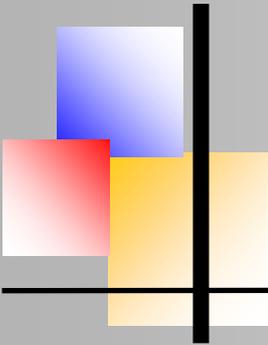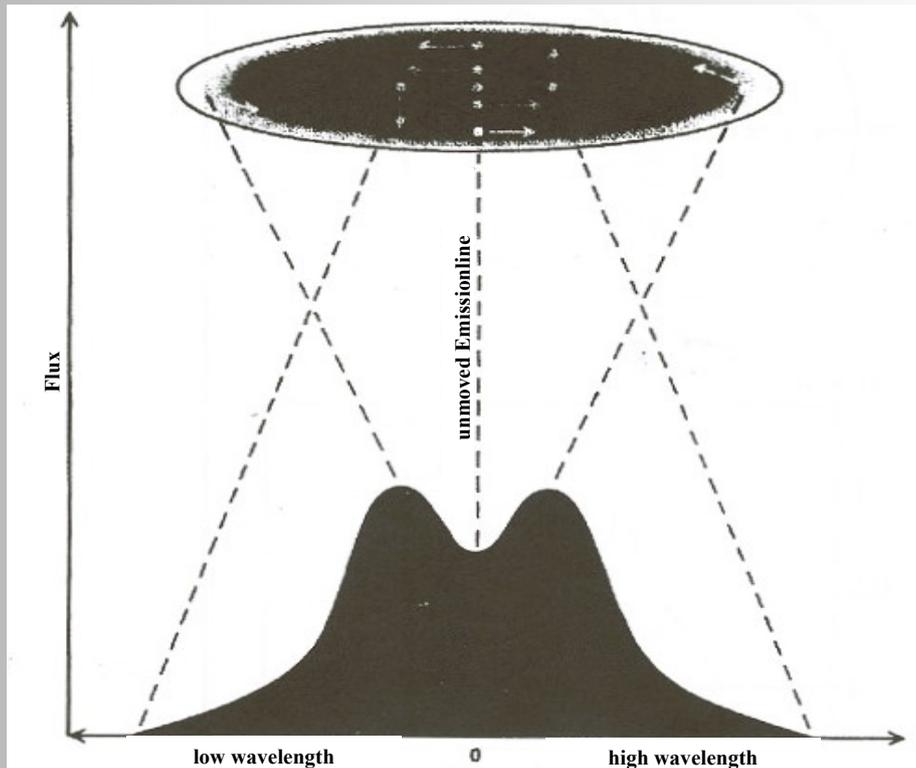
Fig. 3: Kinematic formation of emission lines by the Doppler effect

The radiation of the line appears to be shifted to smaller or larger wavelengths as a result of the disk rotation, depending on whether the emitting areas of the disk are moving towards or away from the observer. The innermost areas of the disk rotate the fastest, causing the largest line shifts, but because of their small volume, they contribute little to the line profile. Gas moving across the line of sight does not produce line shift Fig. 3).

Fig. 4 serves to explain the double peaks, in which the connection between the velocity structure in the circumstellar disk and the profile shape becomes clear. Lines of the same projected radial velocities of the shell particles are drawn into the schematic disc shape, which is viewed "pole-on" in Fig. 4. The length of a line is proportional to the number of particles and thus to the emission intensity (i.e. to the radiant flux) at this radial velocity. However, the relationship between the radiant flux and the radial velocity is given precisely by the velocity spectrum, which is shown in the lower part of Fig. 4. The vertical lines in the profile correspond to the lines in the disk and mark the radial velocities normalized (to v sin i) in steps of $0.1 * v$ sin i. The lengths of the corresponding lines in the profile and in the pane are exactly proportional to each other.
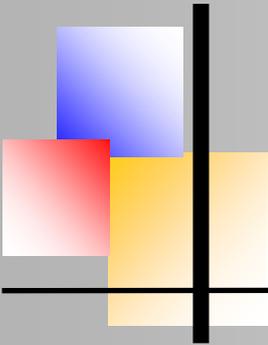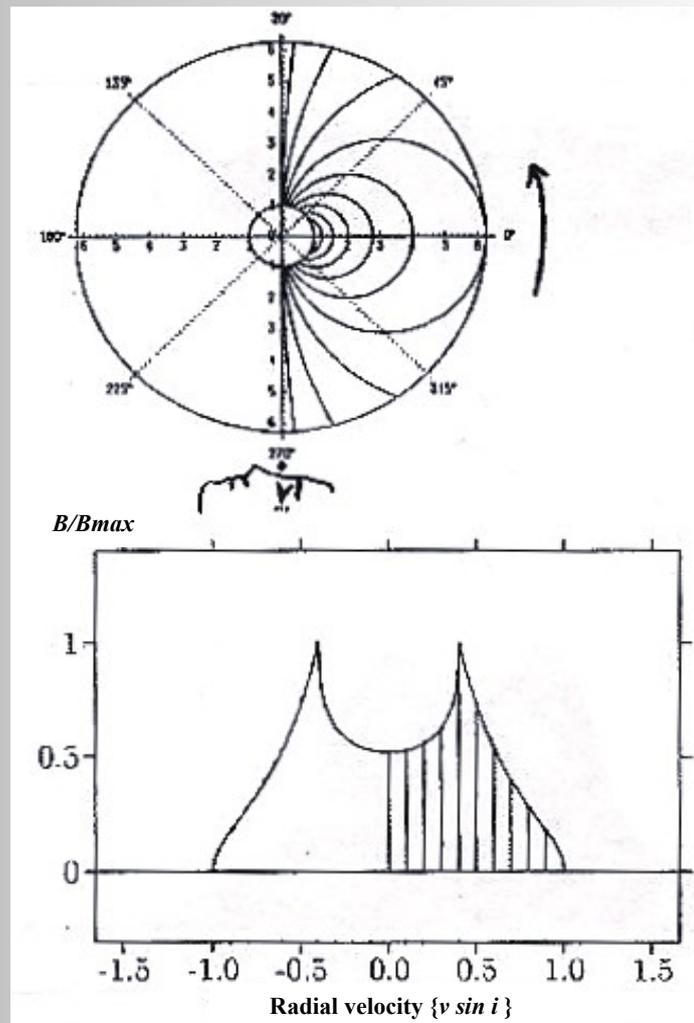
Fig. 4: Development of the double peak structure of emission lines in rotating disks
(from: Hoffmann, D.; diploma thesis, University of Bochum [1995])

According to Kepler's law, the inner structures in the disk correspond to the highest speeds, which are on the outside in the profile. The radial velocity line in the disk that exactly touches the radius of the disk is the longest line due to the finite extent of the disk, so that at this radial velocity there is exactly one peak in the velocity profile. This is because lines at lower projected radial velocities necessarily extend over a smaller area of the disc and are therefore just as shorter as lines at greater radial velocities because these are practically cut off by the edge of the disc (see Fig. 4).Overall, a broadened profile with a central depression and two maxima (symmetrical double peak profile) arises from a purely kinematic consideration.
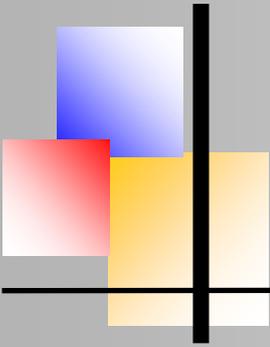
1.4.3 Superimposition of both mechanisms

Of course, the profiles actually observed provide a superimposition of several effects, whereby the dominance of the individual mechanisms is also noticeable in the spectrum. If one performs the convolution between the kinematic profile and the incoherent scattering (radiation transport profile), which is particularly important for optically thick lines, one obtains the so-called wine bottle profiles (Fig. 5). The characteristics of such structures also depend significantly on the angle of inclination i.

Cinematic effects   **Radiation limited**   **Convolution**
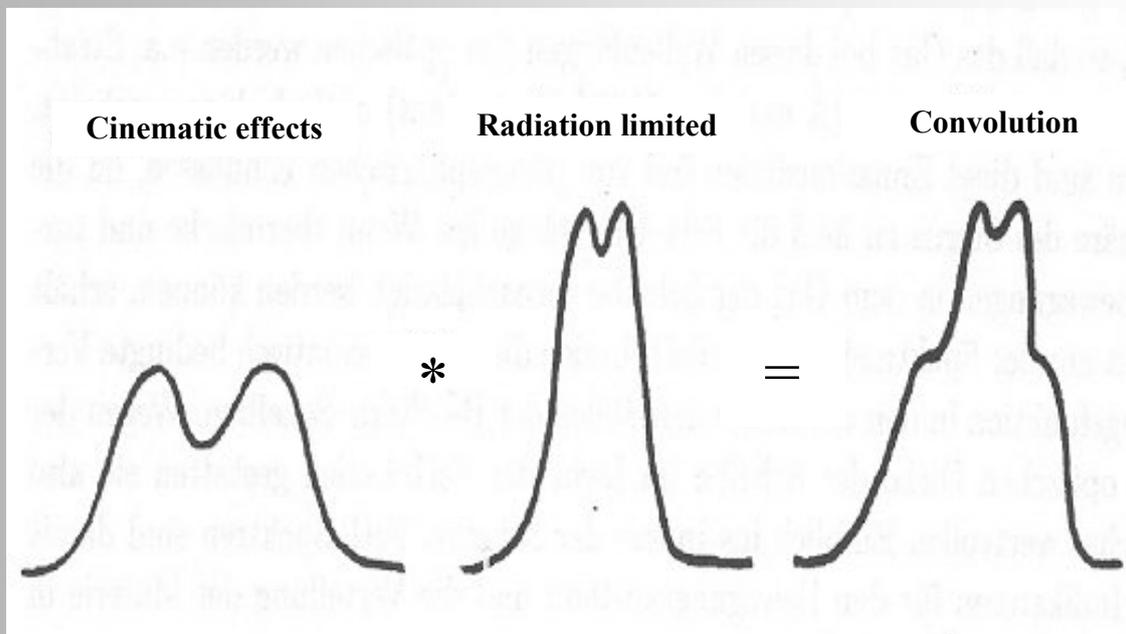
Fig. 5: Convolution between kinematic and radiative transport profile
(from: Dietle, O., diploma thesis Bochum [1993])

1.5 The variations of the Be stars

1.5.1 Overview of the observed variabilities

Since their discovery, many Be stars have been systematically examined again and again in long-term observation programs. It turned out that most be stars show significant changes in their spectra over the course of a few years. The strength and shape of the emission lines sometimes change dramatically, often irregularly and in an unpredictable manner.

Photometric variations were also noted for a larger number of Be stars. The brightness variations are often just as dramatic. The connections between the observed spectral variations and the light curves of their brightness variations cannot yet be described using a uniform scheme. Therefore one must classify the Be stars in the class of "irregular variables".
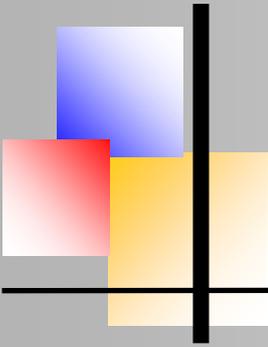
About the properties and problems of Be stars

- The following phenomena occur with the variations of the Be stars, which can also overlap with each other:
- Transitions between a B phase and a Be phase and vice versa (ie formation and loss of a circumstellar envelope)
- Transitions between the Be phases and Be shell phases and vice versa (i.e. strong variations in the thickness of the disk)
- Brightness bursts lasting a few weeks or months, flaring emissions on timescales of days
- Short-term periodic variations in the spectra and fast periodic brightness variations
- Long-term variations in the spectrum, so-called cyclic V/R variations
- Variations due to eclipse variability in binary systems

1.5.2 Cyclic V/R Variations

For many Be stars, the emission line profiles temporarily have the form of asymmetric double peaks (examples in the following Fig. 6). To characterize the asymmetry, the maximum intensity of the short-wavelength peak of the line (in units of the intensity of the neighboring continuum) is denoted by V (violet) and that of the long-wavelength peak by R (red). In the velocity spectrum calculated using the Doppler formula, the V peak is always found at negative velocities, i.e. in the left part of the spectrum (movements towards one another are defined with a negative velocity sign), while the R peak is in the right part of the spectrum at positive velocities. The direction of the asymmetry is described by the quotient of the intensities V/R.
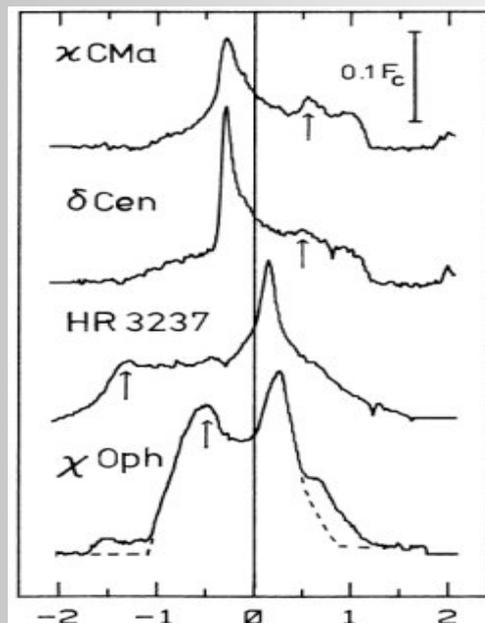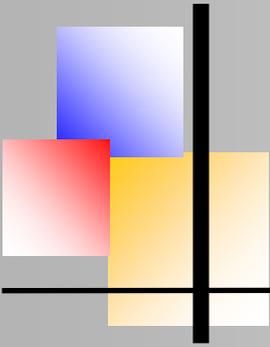

Fig. 6: Examples of asymmetric profiles, abscissa is scaled in units of v sin i. The arrows indicate the positions of the V and R peaks (from: Hanuschik, A&A, 1988, 190, 196).

About the properties and problems of Be stars

The long-term analysis of many Be spectra now shows that the V/R asymmetries of typical double-peak profiles usually show the same direction for a few years, but then often turn in the opposite direction and remain in this direction for a few years, until finally another Reversal of the asymmetry in the first observed direction occurs. The period length of consecutive cycles of such V/R variations are i.a. not strictly constant and also vary noticeably with different Be stars. Mean cycle times are between a few years and a few decades [14].

The cyclic variations in the relative double peak intensities are usually associated with corresponding cyclic variations in the radial velocities of the intensity maxima and the central absorption components of the profiles. The brighter emission peak seems to move towards the middle of the line with increasing intensity [10].

Various models have been proposed to interpret the striking V/R variations of many Be stars:

1. Expansion contraction model
The circumstellar envelope goes through successive cyclical expansion and contraction phases, so that the spectra pulsate with it. With the expansion you get V/R <1, with the contraction V/R >1. This notion was first proposed by Mclaughlin (1962).

2. Model of the elliptical gas ring
According to Shu-Shu Huang [15], the disk is an elliptical ring of gas that precesses in the gravitational field of the oblate star. The precession period corresponds to a V/R cycle. However, the stability of such a configuration remains problematic. A discussion of this idea can be found in Hanuschik [16].

3. Binary Star Hypothesis
The formation of the disk is explained by the mass overflow from the Be star to the companion star. The V/R cycle then corresponds to the orbital period of the binary star system. However, as already explained in Section 1.3.1, one can assume that most Be stars are single stars and therefore obey mechanisms other than the interaction with a companion star.

4. Star Wind Model
Variable stellar winds can result in variable mass overflow onto the gas disk. When this matter interacts with the cool gas disk, significant disruption in the disk can occur. However, it must be doubted whether these disturbances can be of a periodic nature.
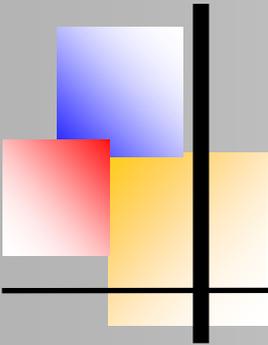
5. Model of a density wave

A disturbance in the density distribution of the Kepler disk is assumed to explain the asymmetrical profiles. In 1991, Okasaki formulated the idea of a wavy density perturbation that circulates in the differentially rotating disk [17]. Such a disturbance would manifest itself as a redistribution of the matter in the disk, so that more particles contribute to the radiation flux on the side of the shell with the increased density than on the side with the reduced density. This would lead to a large imbalance in the number of particles moving towards and away from the observer, and therefore to asymmetric velocity spectra. An illustration of this idea is shown in Figure 7 below. The disc shown is moving in a counter-clockwise direction.
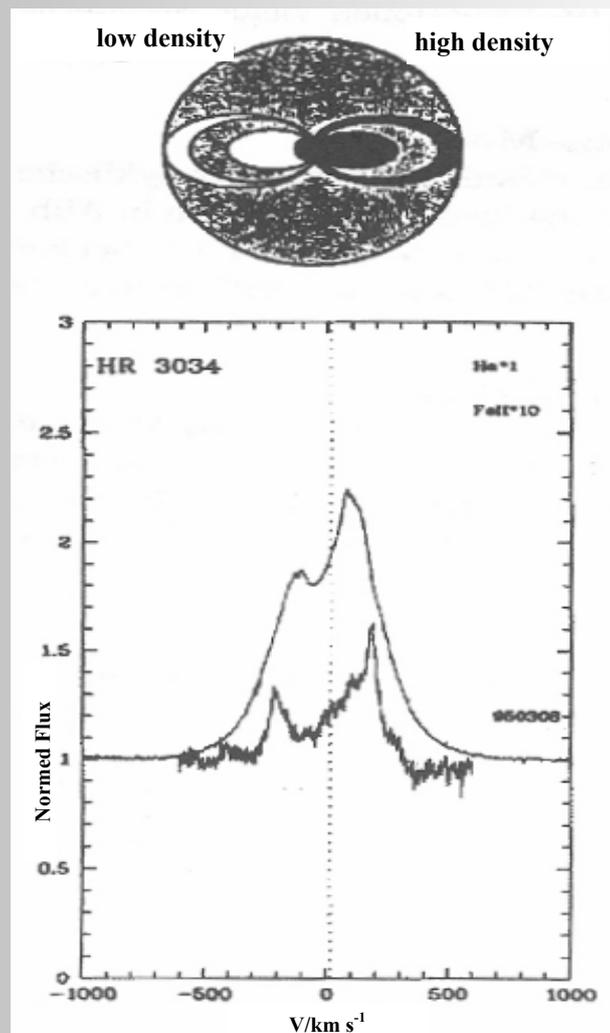
Fig. 7: Cause of profile asymmetries due to density disturbance
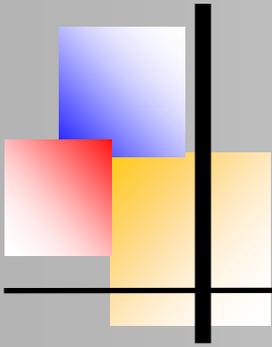
About the properties and problems of Be stars

The cause of the sometimes dramatic irregular brightness variations in Be stars could also be found in the increase and decrease in density perturbations in the surrounding gas rings, possibly in connection with instabilities in the outer layers of the rapidly rotating central stars. The parameters of this model approach are determined on the one hand by direct analysis of the observed spectra and on the other hand by physically meaningful boundary and secondary conditions.

Be stars are relatively close hot main sequence or giant stars that are easy to study due to their brightness. As has been shown here, the disks around Be stars are not continuum sources but emit line radiation. Statements about the distribution and the state of motion of the gas in the disk can be obtained from the shapes of these emission lines, which are essentially determined by the Doppler effect. Be stars therefore represent an ideal laboratory for understanding stellar accretion disks.

Literatur

[1] Dachs, J., Sterne und Weltraum 1995, 11, S. 798

[2] Slettebak, A. The Be-Stars, Space Science Reviews, 1979, 23, 541

[3] Snow, T., Astrophys. J. Suppl., 1982, L39, 153

[4] Scheffler H., Elsässer H., Physik der Sterne, BI-Wiss.-Verl., 1990, S. 187

[5] Slettebak A., Astrophys. J. Suppl., 1982, 50, 55

[6] Slettebak A., IAU Symp. 1976, Nr. 70, 123

[7] Hanuschik R. W., A&A, 1996, 308, 170

[8] Dachs J., Engels D., Kiehlin R., A&A, 1986, 194, 176

[9] Kzriz S., Harmanec P., Bull. Astron. Inst. CSSR, 1975, 26, 65

[10] Hanuschik R.W., Hummel W., Sutorius E., Dietle O., Thimm G., A&A 1996, 116, 309

[11] Baade D., in: Physics of Be-Stars (IAU Coll.92), 1987, 361

[12] Bjorkman J.E., Cassinelli J.P., Astrophys. J., 1993, 409, 429

[13] Hummel W., Dachs J., A&A, 1992, L17, 262

[14] Hanuschik R.W., Hummel W., Sutorius E., Dietle O., A&A, 1995, 300, 163-176

[15] Huang, S.S., ApJ, 1973, 183, 541

[16] Hanuschik, R.W., A&A, 1988, 190, 195-197

[17] Okasaki, A.T., Pub. Astron. Soc. Japan, 1991, 43, 75-94
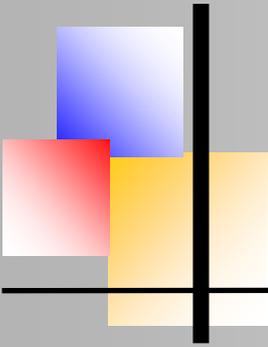
VV Cephei – Campaign after Eclipse 2018

Ernst Pollmann (ernst-pollmann@t-online.de)

Abstract

None of the studies or work published so far has been able to clearly demonstrate which of the individual components of the binary system VV Cephei, such as the B companion, the accretion disk or the emission lobes, produces the residual Hα emission during the phase of total eclipse. The model recently proposed by Pollmannn & Bennett suggested that only the upper emission lobe (blue emission V of the Hα components), which is bound with the rotation axis of the B companion star and its accretion disk can be solely responsible for this residual emission. *Part I*: With continued observations 4 years after the end of the eclipse in December 2018, we found that from the partial eclipse of the emission lobes and the total eclipse of the B star plus disk through the M star, the Hα EW with the period of 43 days and the significantly smallest amplitude (compared to the EW of the following later sections) explaines the residual emission. *Part II* documents the duration of the partial eclipse of the Hα emission flux (components V+R) as well as the total UV flux eclipse through the M star and the analysis of the quasi-periodic variations of their time behavior. *Part III* describes the period analysis of the V/R variations from November 2000 to February 2023. The sinusoidal amplitude of the linear detrended V/R data of the two emission lobes V and R in Fig. 10 clearly demonstrates the Kepler orbital period of 7430 days with an average amplitude of (+/-) 0.33.
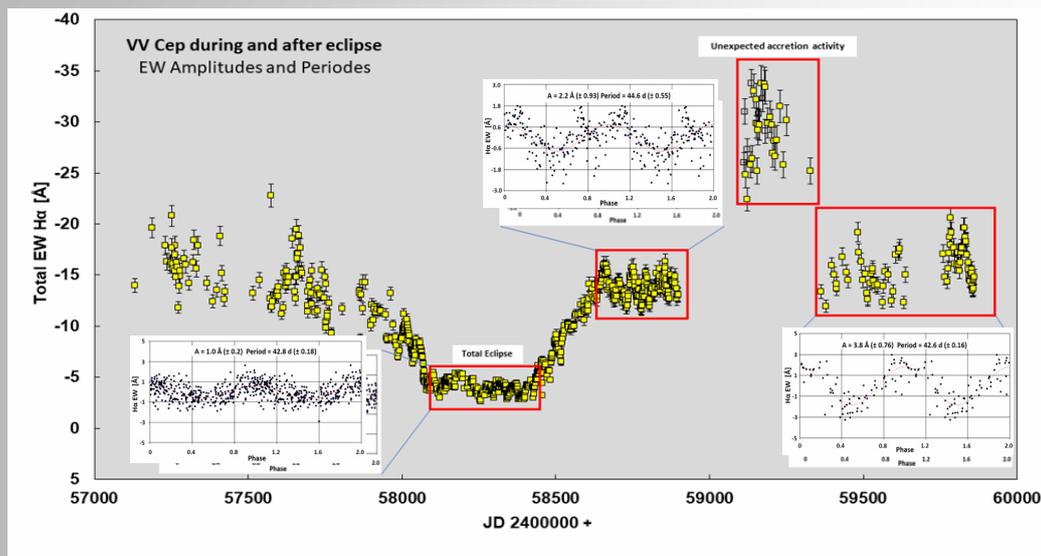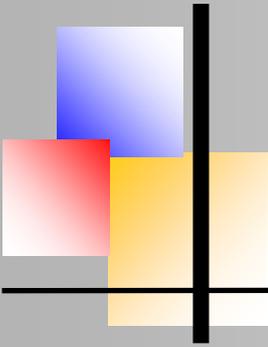

Fig. 1: Overview of the campaign to detect the rotation axis precession of the B star with

VV Cephei - Campaign after Eclipse 2018

In this project it was particularly important to use a uniform evaluation program to determine the Hα-EW in the spectra of different observers, which were obtained with different spectrographs, i.e. with different spectral resolutions between 10000 and 20000. This heterogeneity required a high level of accuracy in uniform wavelength scaling, normalization of the continuum, and fixed definition of the EW integration region. These requirements are given by using the program SPECTRO-CALC (https://www.astrophoto.at). Figure 2 describes the EW integration range as well as the spectral lines that were used for the uniform post-calibration of all spectra.
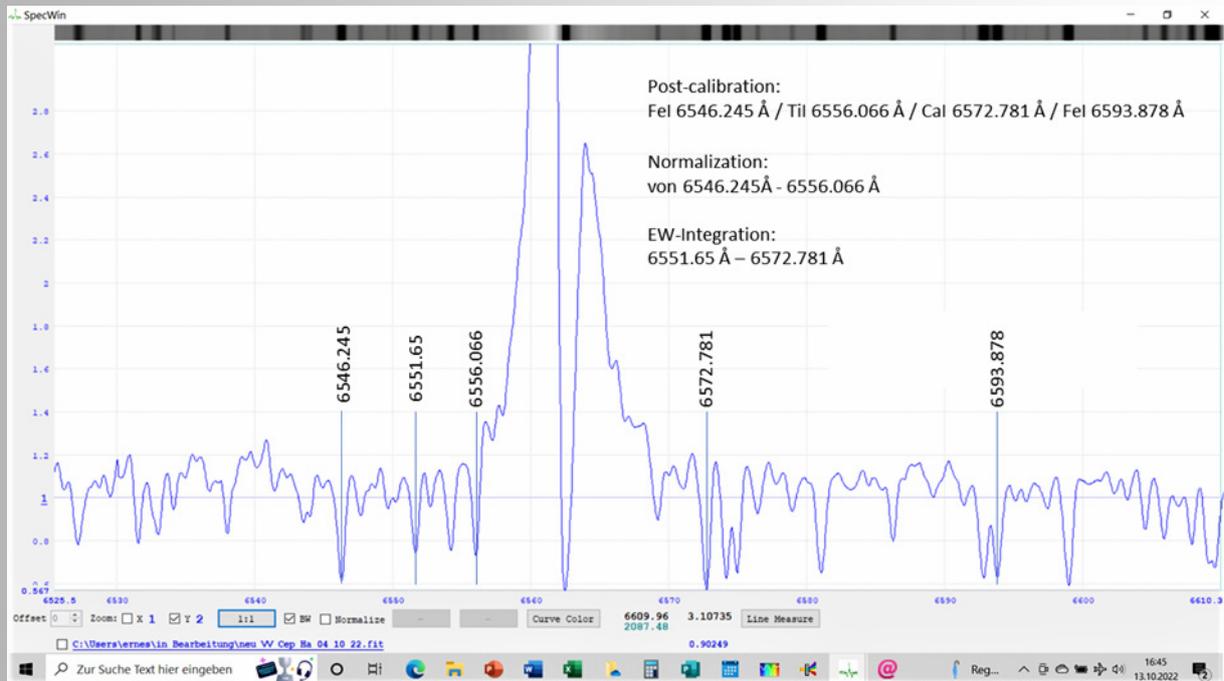
Fig. 2: Description of selected wavelengths for recalibration, continuum normalization and the EW integration range.

The wavelength calibration was carried out at the wavelengths FeI 6546.245Å / TiI 6556.066Å / CaI 6572.781Å / FeI 6593.878Å recommended by Hutchings & Wright (1971) as suitable in the spectrum of the M supergiant. The normalization was performed in the range of 6546.245Å - 6556.066Å.

The EW integration area extended from 6551.65Å – 6572.781Å. The measurement accuracy of the wavelength calibration was consistently in the range of (±) 0.005Å. The accuracy of the determination of the EW can be given as (±) 0.3Å in terms of reproducibility measurements. In this respect, precise prerequisites were given with which the project could be carried out.
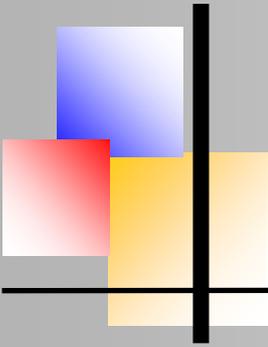
Results

In the following, the analyzes of the periodicity and amplitudes of the Hα-EW will be presented. First, Figure 3 describes the phase diagram of the period analysis of the total eclipse section of JD 2458068-58441. With a period of 42.8 d (± 0.18), the Hα-EW varies with an amplitude of 1.0 Å (± 0.2).
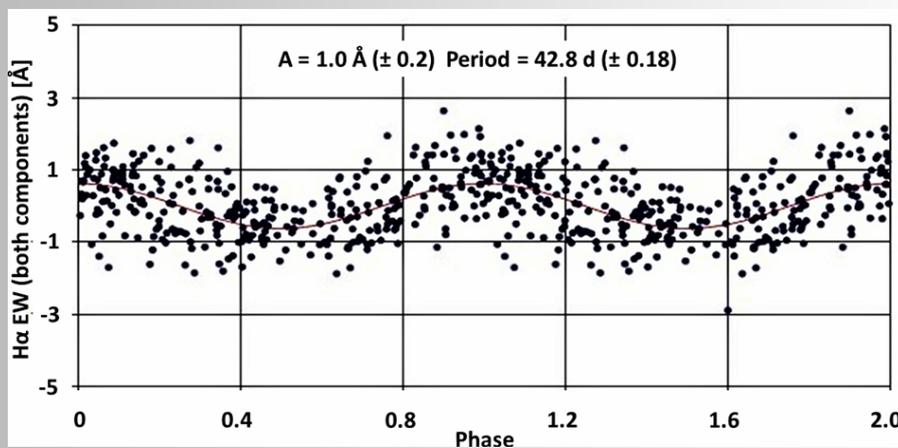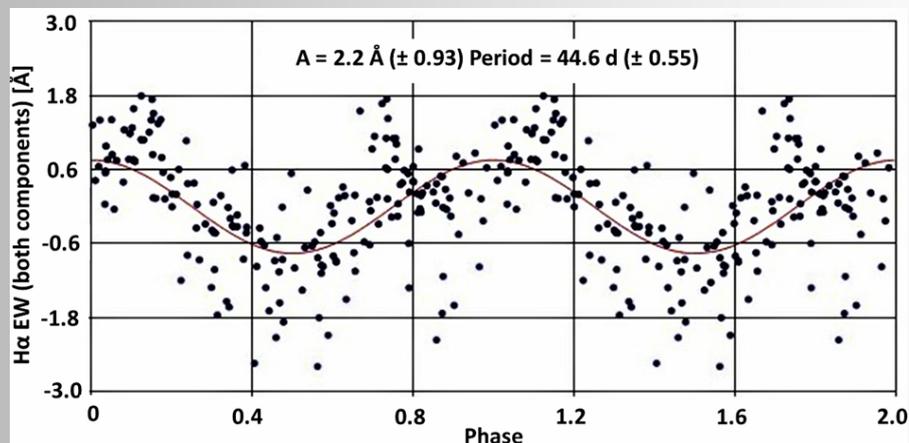

Fig.3: Evaluation of the Hα-EW period and the amplitude for the section of total eclipse of JD 2458068-58441 (see also Fig. 1)

Figure 4 describes the phase diagram of the periodicity and amplitude of the Hα-EW for the section JD 2458663-58897 outside the total eclipse. With a period of 44.6 d (± 0.55), the Hα-EW varies with an amplitude of 2.2 Å (± 0.93).

Fig. 4: Evaluation of the Hα-EW period and the amplitude for the section outside the total eclipse of JD 2458663-58897 (see also Fig. 1)

VV Cephei - Campaign after Eclipse 2018
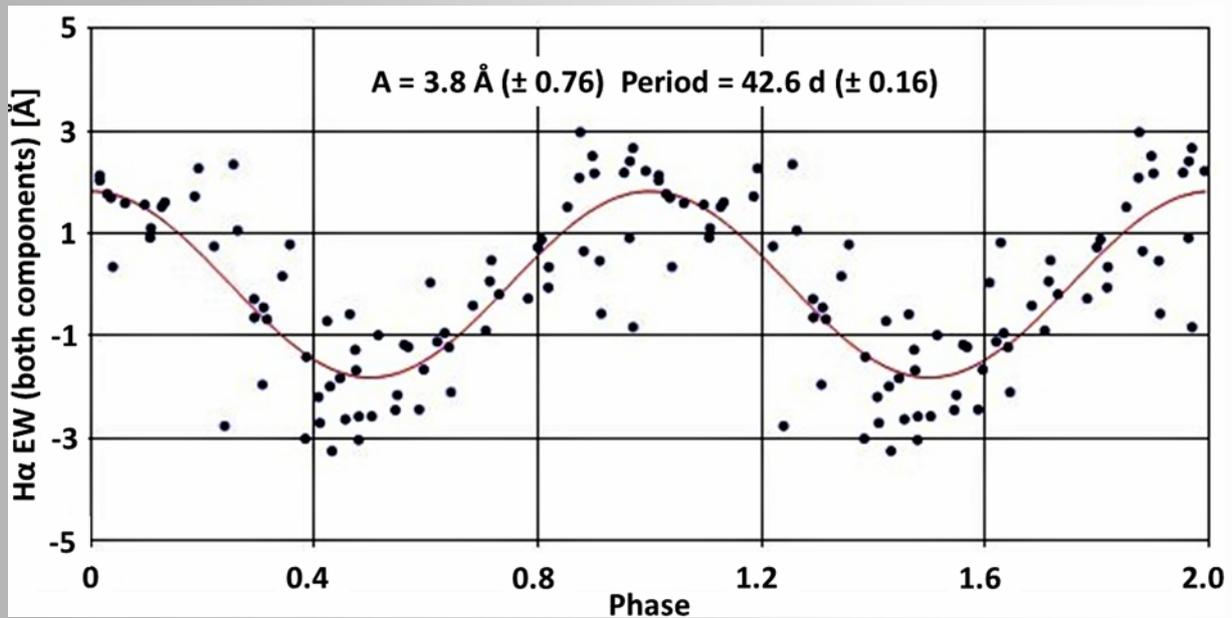
Fig. 5: Evaluation of the Hα-EW period and the amplitude for the section outside the eclipse of JD 242459363-59637 (see also Fig. 1)

The data of these three periods analyzes are summarized in the table below:

Time section	Hα-EW Amplitude [Å]	Period [d]
JD 2458068-58441	1.0 (± 0.2)	42.8 (± 0.18)
JD 2458663-58897	2.2 (± 0.93)	44.6 (± 0.55)
JD 2459363-59637	3.8 (± 0.76)	42.6 (± 0.16)

For the investigation period JD 2458068 to JD 2459637 (= 4.3 years) an average period of Hα EW of 43.3 days (± 0.3) was found. This is also their typical period because of the coupling of the two emission lobes with the rotational axis of the B star.

Fig. 6 shows the Hα line flux of both emission components V+R along with UV flux represented by Umag measurements. In the U-band, most of the flux is believed to come from the hot components of the binary system - the B star and its precessing accretion disk. Umag brightness measurements during the phase of the _total eclipse_ documents almost the complete disappearance of UV flux of the B star plus its accretion disk by the M star.
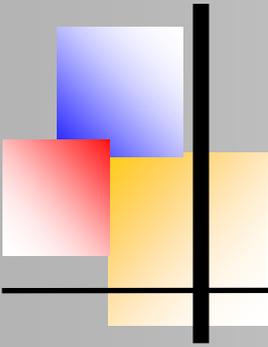
VV Cephei - Campaign after Eclipse 2018
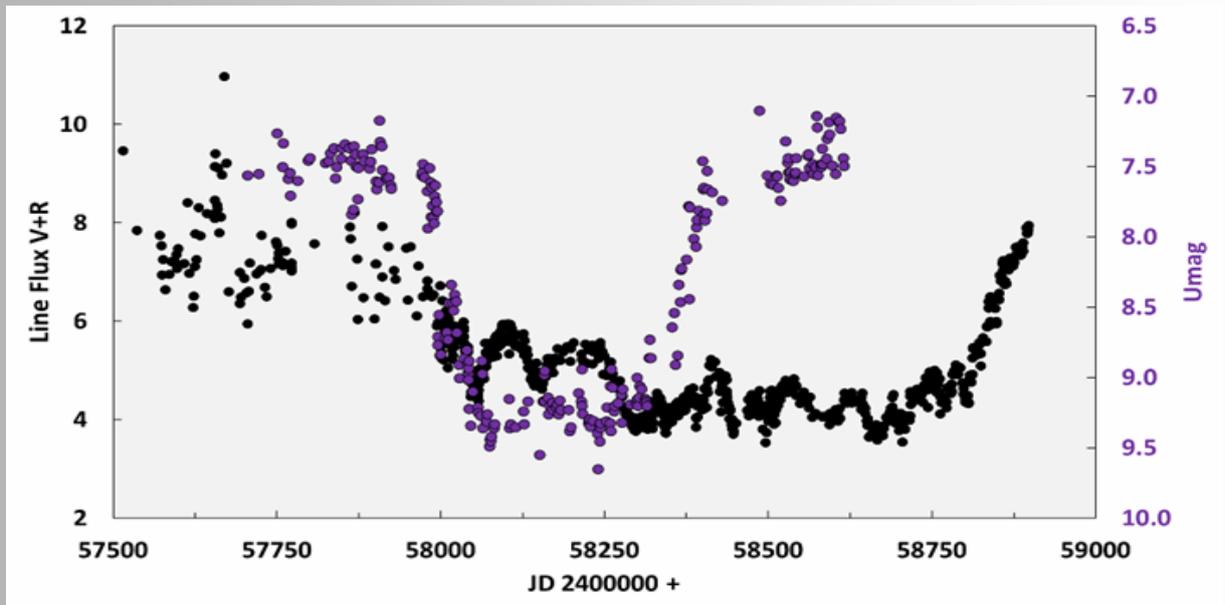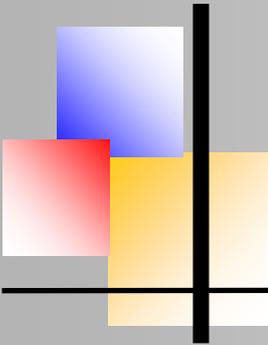
Fig. 6: *Total eclipse* of the B star plus disk (JD 2457972-58486) represented by Umag (https://bav-astro.eu/index.php/veraenderliche/bedeckungsveraenderliche/vv-cep-kampagne) and *the partial eclipse* of the Hα line flux of the emission components V+R (JD 2457500-58895)

But in the observer's line of sight, the emission sources V+R, and their coupling to the rotation axis of the B star, extend far beyond the diameter of the supergiant, resulting only in a partial eclipse by the M star. Contrary to our earlier assumption, we can say now, that the partial eclipse of the components V and R by the M star is responsible for the residual emission during the total eclipse.

Both fluxes, Hα (V+R) as well the UV (B star plus disk), are subject an additional orbital precession of the rotation axis of the B star. This is easy to recognize as quasi-periodic variation of its time behavior in Fig. 6. A period analysis of its detrended data is shown in Fig. 7a-d.

The Umag analysis of the polynomially detrended data (degree 15) in figure 7b results in a period of 162.5 d (±3.5). The analysis of the detrended V+R data in figure 7d results in a period of 151.2 d (±1.0). The average period from both thus leads to 157 d. The difference of about 10 days between these two periods is most likely due to the relatively small amount of Umag data.
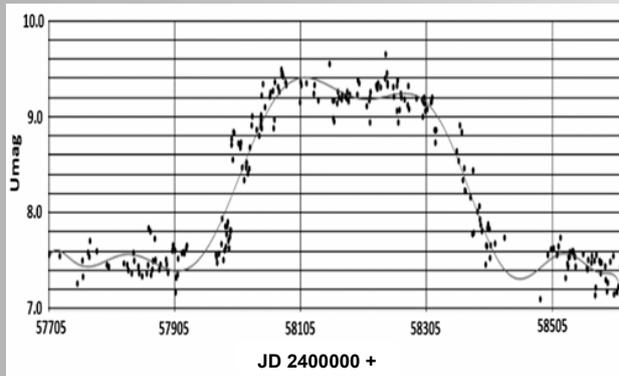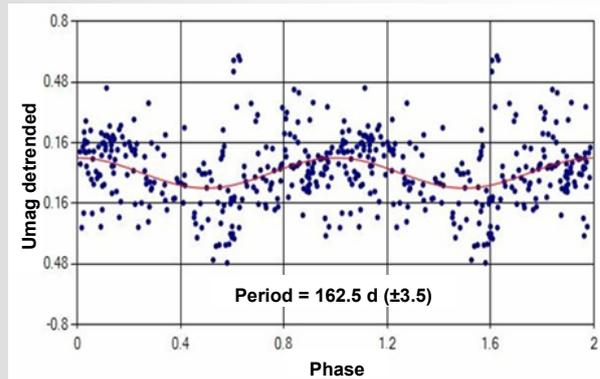
Fig. 7a: Umag measurements during total eclipse

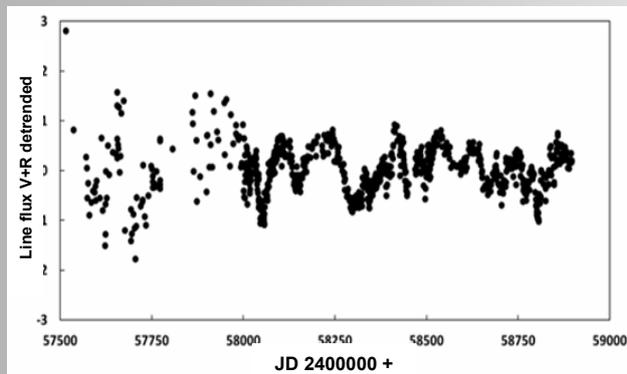**Fig. 7b:** Umag period analysis of the polynominal (degree 15) detrended data of Fig. 7a P = 162.5 d (±3.5)

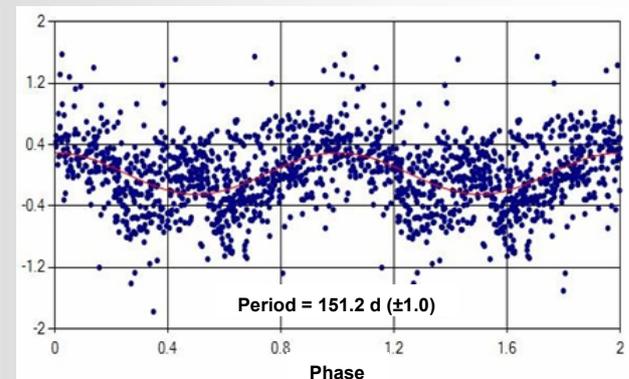**Fig. 7c:** Hα line flux V+R polynominal (degree 3) detrended

Fig. 7d: Period analysis of the detrended data in Fig. 7c; P = 151.2 d (±1.0)

Note that the 43d EW period is about ¼ of the 162.5 d period. It is not clear yet how this is to be interpreted. Observations during the following orbital sections of the B star may lead to an explanation.

Part III

The 43.3 d EW period of the blue (V) and red (R) emission lobes described in Part I and their coupling with the precessing rotation axis of the B star naturally led to the question of their behavior in the orbital phases periastron and apastron. Figure 8 shows the monitoring of the V/R ratio of the first campaign from November 2000 to February 2023. The blue stripes mark the orbital phases periastron and apastron with a period of 7430 days (Wright, 1977).
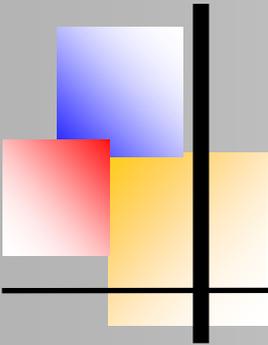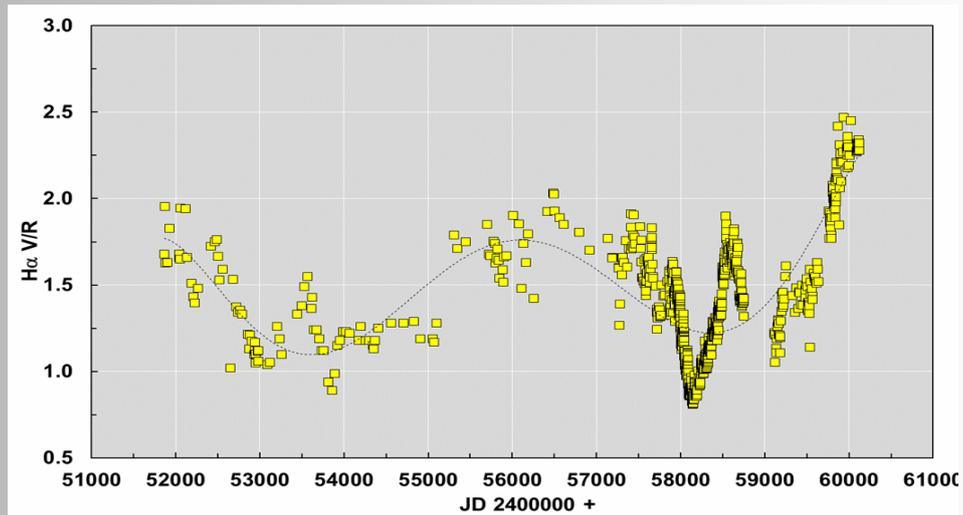
Fig. 8: Time behavior of the ratio V/R of the first campaign
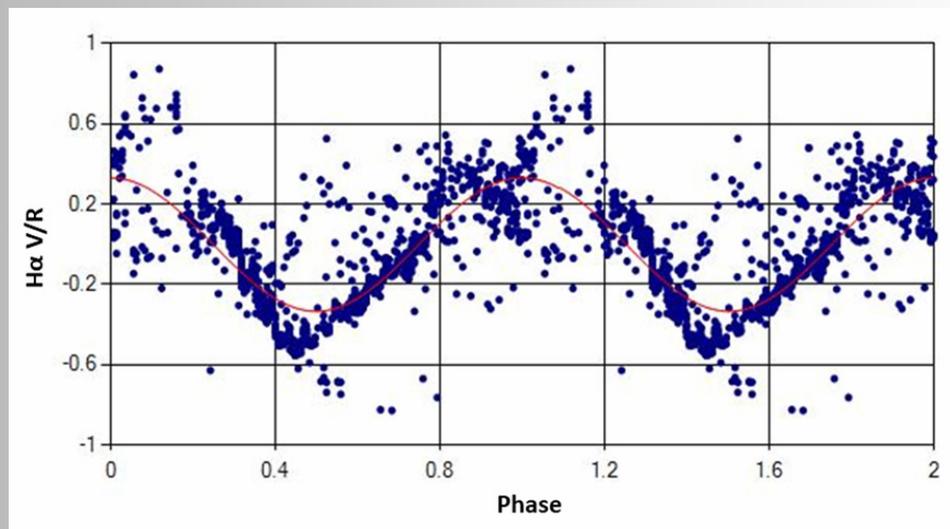November 2000 to February 2023

Fig. 9: Phase diagram of the campaign November 2000 to February 2023;
Period = 7443d (Wright 1977; P = 7450d; T = 2438389 (± 60)

To demonstrate the ratio V/R in the B star's Kepler-orbital context, a period analysis was performed of the polynominal detrended data in Figure 8. In the sinusoidal phase diagram of this analysis in Fig. 9 (red curve), the periastron has to be assigned at phase 1.0, the apastron at phase 0.5.
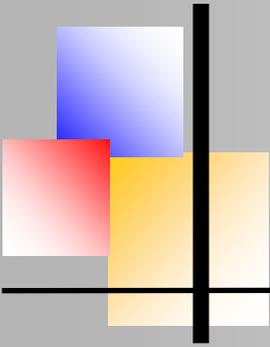
Conclusion

With the present, renewed investigation campaign, the precession period of 43.8 d (± 0.1) derived from the radial velocity of the blue emission component published by Pollmann (2022) is very well confirmed with the averaged Hα-EW period of 43.3 d (± 0.3) during the total eclipse as well as out of the eclipse.

The tabular comparison of the Hα-EW amplitudes also shows that, contrary to the assumptions of Pollmann & Bennett (2020), the observed residual emission during the period of the total eclipse (JD 2458068-58441) have been generated from both emission lobes (V+R) in the disk rotation axis of the B star.

The coupling of the emission sources V+R with the rotational axis of the B star extends far beyond the diameter of the supergiant in the observer's line of sight. This results in only a partial eclipse through the M supergiant, and hence to the residual emission during the total eclipse. This claim is strongly supported by photomultiplier brightness measurements in U, which support the complete disappearance of the B star during the total eclipsing phase.

Continued monitoring the B star's approaching periastron phase in 2025 will determine the effect of the precession of the B Star's rotation axis and whether it can be observed in this form in further orbital phases The sinusoidal amplitude of the linear detrended V/R data of the two emission lobes V and R in Fig. 9 clearly demonstrates the Kepler orbital period of 7430 days with an average amplitude of (+/-) 0.33.

The precessing rotation axis of the B star with the coupled emission components V and R is characterized by two superimposed periods: the short-term precession period with P = 43 days and an (averaged) precession period with P = 157 days. The present results imply that both periods remain during a complete orbit of the B star. Although the 43-day period of the B star's rotation axis is triggered by the M supergiant, the excitation process for the 157-day period remains unclear.

Acknowledgement

References

Hutchings, J. B., and Wright, K. O., 1971, Mon. Not. Roy. Astron. Soc., 155, 203.
Pollmann, E., and Bennett, P. D. 2020, J. Amer. Assoc. Var. Stars, 48
Pollmann, E., 2022, J. Amer. Assoc. Var. Stars, 50
SPECTRO-CALC (https://www.astrophoto.at)
Wright, K. O., 1977JRASC..71..152W (harvard.edu)
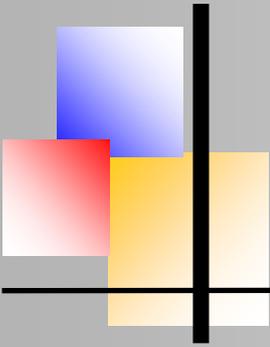
Comet C/2022 E3 (ZTF) – Spectrum and its elements

Michael Koenig, www.astro-images.de

On January 29, 2023, I managed to capture a well exposed spectrum of comet C/2002 (3) (ZTF). As it turned out, not the brightness was the problem, but the fast motion of the comet in the sky. This presented special software challenges for tracking the comet's nucleus "on the slit" of the LISA spectrograph.

The normally used tracking velocities in RA and DE are +/- 1 of the sidereal velocity. This was much too slow for the comet, because although tracking was done in both axes, the nucleus loosely left the slit behind. Only at 4x speed was it possible to fix the slit on the bright nucleus of comet C/2002 E3 in the field of view, which measures only a few minutes of arc.

It was quite unusual with this setup, that the stars in the field of view of the guider are moving fast through the guider images - relative to the fixed comet nucleus. There were also cases where the comet covered a star before it then emerged again from the bright core area. This was an unusual scenario - because otherwise my sources usually behave rather statically during imaging. To record the spectrum, I made several individual exposures. I started with 5-minute exposures but was not satisfied with the signal-to-noise ratios. So, I increased to an exposure time of 30 minutes. The spectrum combines 5 of these individual exposures.
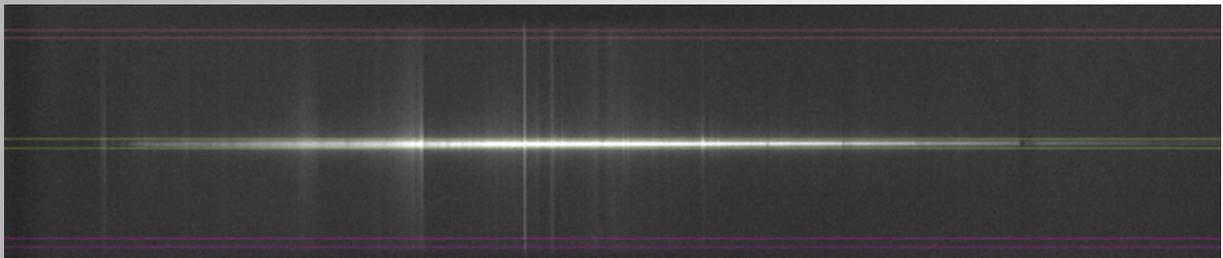

Fig. 2: Raw spectrum of comet C/2022 E3 (ZTF); The bright spectral stripe in the center is from the comet nucleus. The vertical lines are emission lines (bright) and absorption lines (dark) coming from the comet or Earth's atmosphere.

The spectral profile shows a continuum along which emission lines and absorption lines can be seen as structures. The continuum can be well described with a polynomial fit. The following image shows the spectral profile at the top and the derived continuum in the middle. If you now divide the two profiles, i.e., calculate: spectrum / polynomial fit, you get a spectrum that better highlights the "darker areas" in the violet (far left) and in the red (far right).
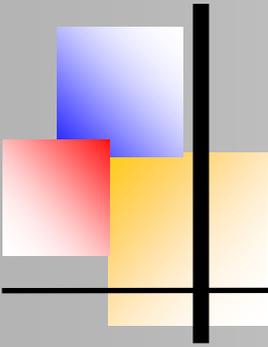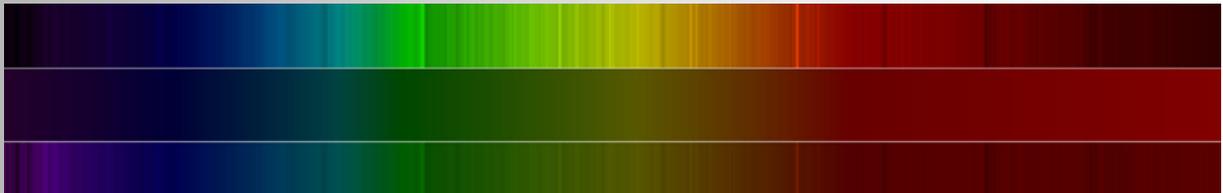
Fig. 2: Colour bands of the spectral profiles: (top) spectrum, (middle) trend line - polynomial of 5th degree, (bottom) difference profile

In the continuum-adjusted spectrum, an intense double line in the violet is particularly striking. This can already be seen in the spectrum with the continuum, but it is not yet clear that this violet line pair is the brightest line structure in the entire comet spectrum. This "violet prominence" becomes even more important, if one considers the typical colour of comets (see article).
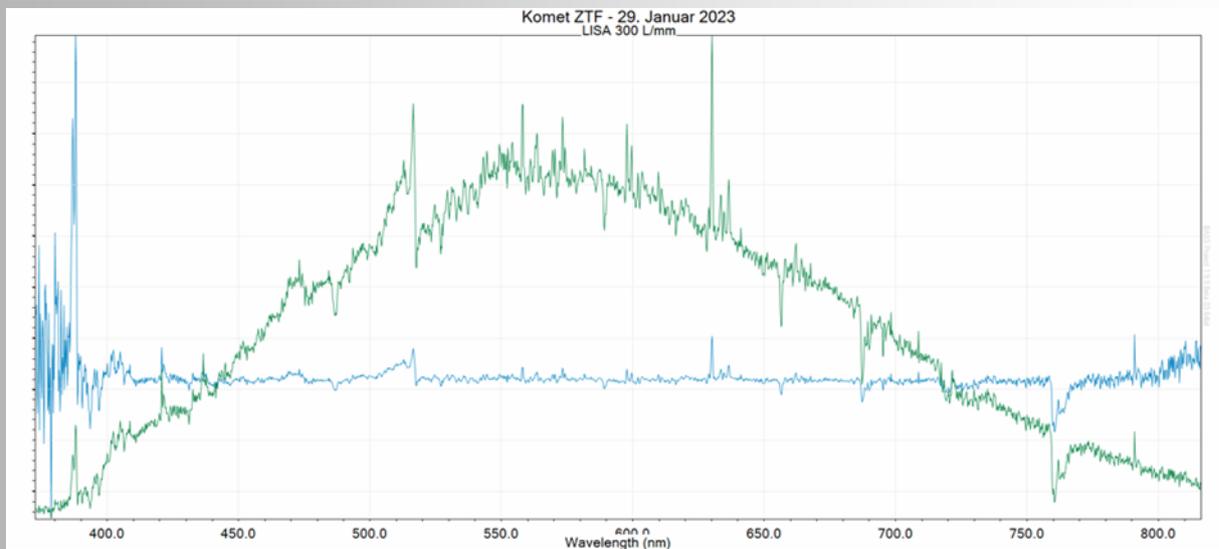

Fig. 3: Spectrum of comet C/2022 E5 (ZTF) - (green) spectrum and (blue) trend-adjusted spectrum.

Now let us have a look at the elements that could be identified in the comet's spectrum. Ahead of this, I would like to share some physical details about molecule spectra. Unlike an atom, which can produce different energy levels through excited states of the electrons in the atomic shell, found in emission and in absorption in the spectra, a molecule offers more options. This is because the total energy of a molecule depends not only on the excited state of the electrons in the shell collective, but also the vibrational states of the bound atoms with respect
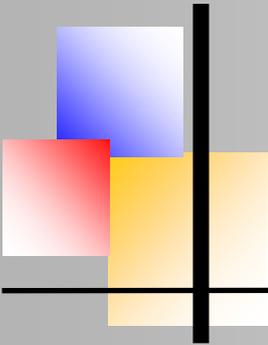
to each other (vibration), as well as the rotation of the entire molecule contribute. These three energy contributions provide distances of the discrete energy levels on different scales. The largest distances result from the energy levels of the shell electrons. These are a few electron volts (eV) and in the optical spectrum these range from the ultraviolet to the infrared. The vibrational states are closer, separated by only a few 0.1 eV. Even closer are the rotational states, which are 100 times denser. Their separation is only a few meV, which corresponds to microwave photons at transitions. All contributions together result in a dense forest of lines, so-called molecular bands.
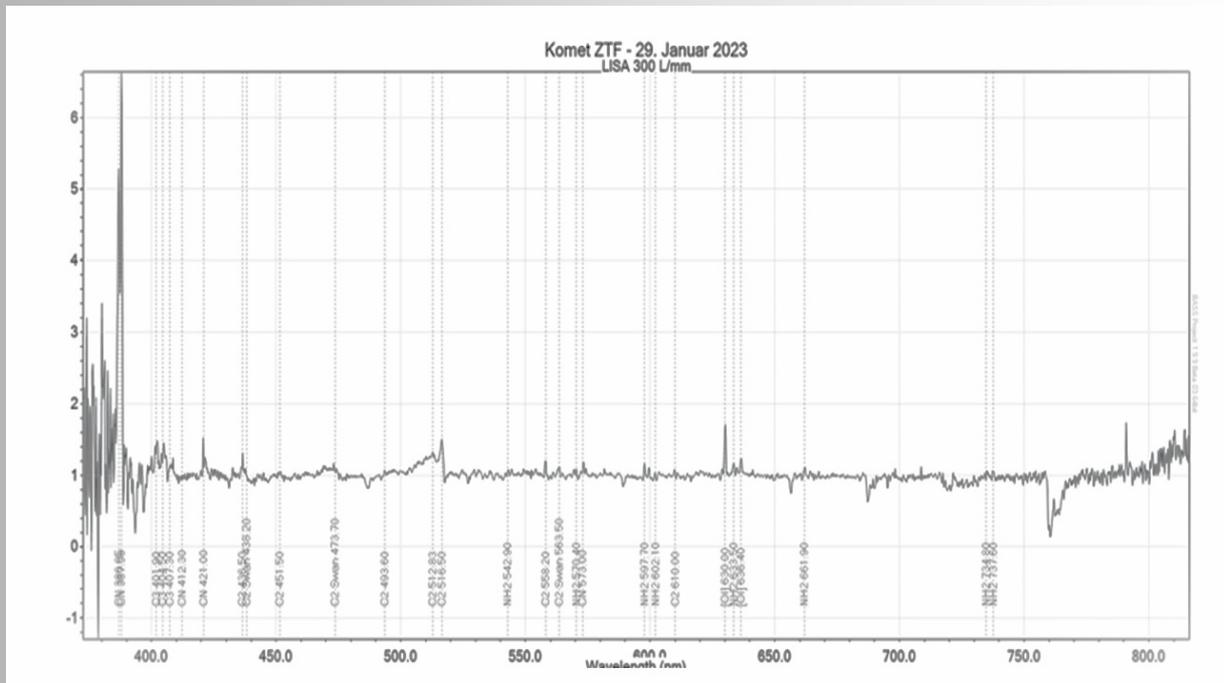

Fig. 4: Spectrum of comet C/2022 E3 (ZTF) - The vertical lines are used to identify the molecules and atoms responsible for each emission contribution or absorption.

In the spectrum of comet C/2022 E3 they show up as "Swan bands". They were first detected by the Scottish physicist William Swan in the 1850s when he studied the spectra of hydrocarbons. That it was the diatomic carbon molecule (C2) was not proven until 1927. By the way, the blue glow of the flame of a burning candle can also be traced back to C2 bands. In the comet spectrum this does not appear clearly, there the C2 bands dominate in the green spectral range. The brightest lines of the spectrum are produced by the CH molecule at about 387 nm in the form of a double line. The striking green Swan band, whose long-wavelength edge is at 516 nm, is only one-third as strong.
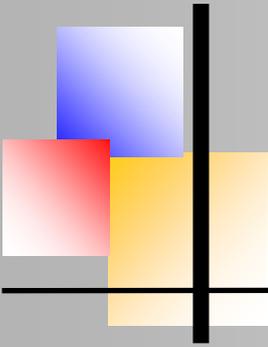
Comet C/2022 E3 (ZTF)

There are individual emission lines in the spectrum whose peak exceeds that of the Swan bands. The [OI] line at 630 nm in the red is striking. This appears in my setup as a single line. Higher resolution spectrographs, give here two, closely spaced lines. Both go back to the forbidden line of the simply ionized oxygen - exactly two different [OI]-light sources: Once the gas from the Earth's atmosphere and once the gas in the comet's coma.

The mini-wavelength difference of these two [OI]-lines measures only a few 10 km/s and is caused by the radial velocity component of the comet's orbit. If you look closely, the [OI] line is slightly red-shifted relative to the rest wavelength plotted in the figure. From this, we can conclude that comet ZTF was moving away from us at the time the spectrum was taken, which was late January 2023. If I had taken its spectrum earlier, when it was moving toward us, relatively speaking, the [OI] comet line would have been detectable on the short wavelength side of the [OI] Earth atmosphere line.
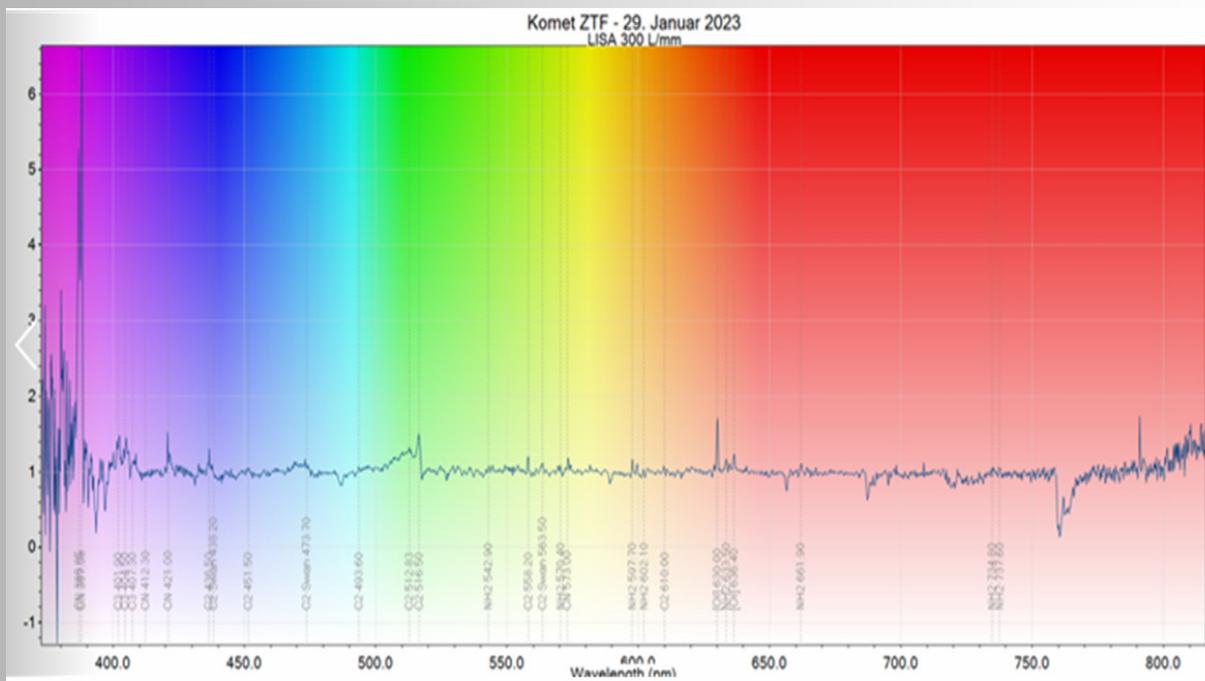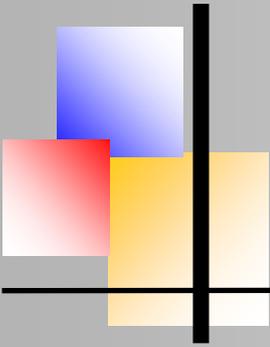

Fig. 5: Spectrum of comet C/2022 E3 (ZTK)
line details with spectral colours in the background.

And here two more enlargements of the spectrum shown above. Once the area of the green Swan band and once the surroundings of the [OI] line. The whole line forest of the band

Comet C / 2022 E3 (ZTF)

spectrum is not resolved in detail here, but you can see well that the many C2 lines originate at shorter wavelengths and their intensity increases by superpositions towards longer wavelengths, so that there is an increase from left to right in the profile. The long wavelength termination of this Swan band is an intensity peak at about 516 nm.
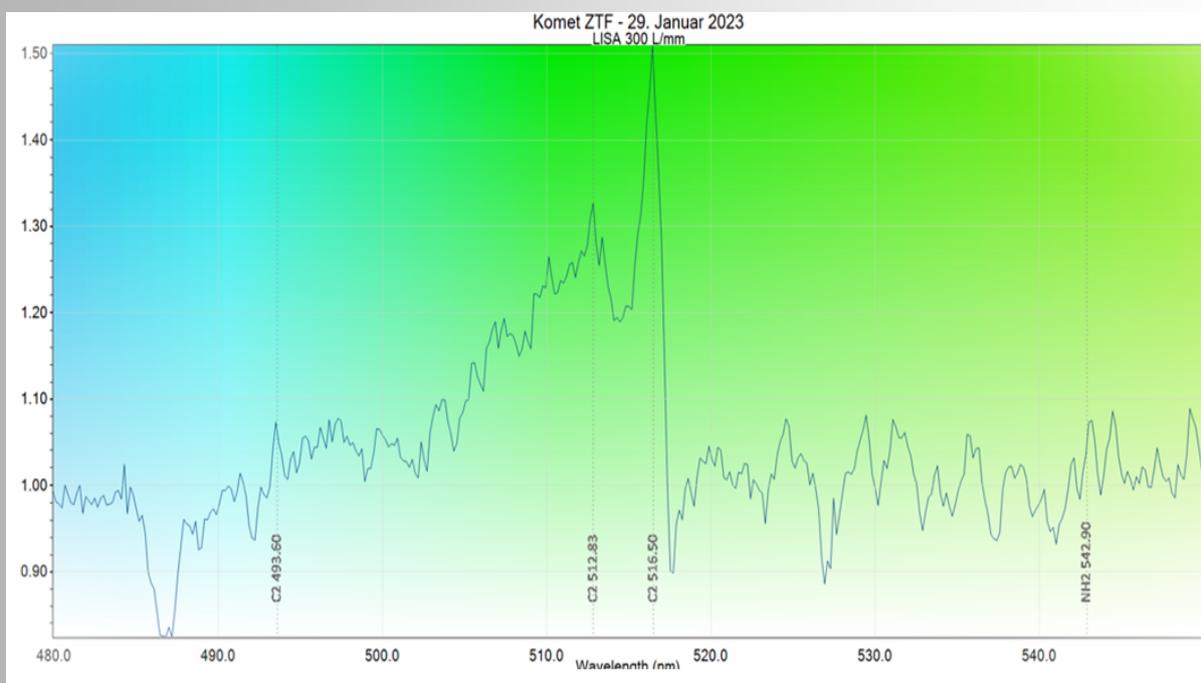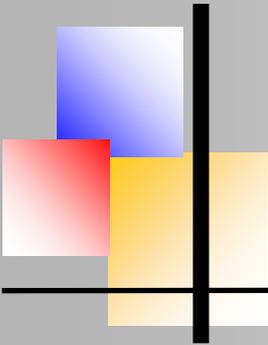

Fig. 6: Comet ZTF_29012023
The long wavelength termination of this Swan band is an intensity peak at about 516 nm.

In addition to the C2 bands, what may be new to some readers is the aspect that C3 molecules are also detected in comets (Fig.7). There are still questions associated with this "tricarbon" as to its origin. Today it is assumed that these polyatomic molecules go back to "parent molecules" which sublime from the comet surface - i.e., are formed during the transition solid > gaseous. In the case of C2, i.e., the dicarbon, C_2H_2 (ethyne) is the parent molecule.

In C3, there is probably no such parent molecule, but the third C atom is added to the compound during photo-dissociation processes, via C radicals. Here many hydrocarbon compounds are involved, which also contain nitrogen, which plays an important role in the element cocktail of the comet, as one can see at the violet CN double lines. In the technical articles one finds as contributors for example C_4H_2 (diacetylene), $CH_2C_2H_2$ (allene), CH_3C_2H (propyne), C_2H_4 (ethene) and HC_3N (cyanoacetylene).
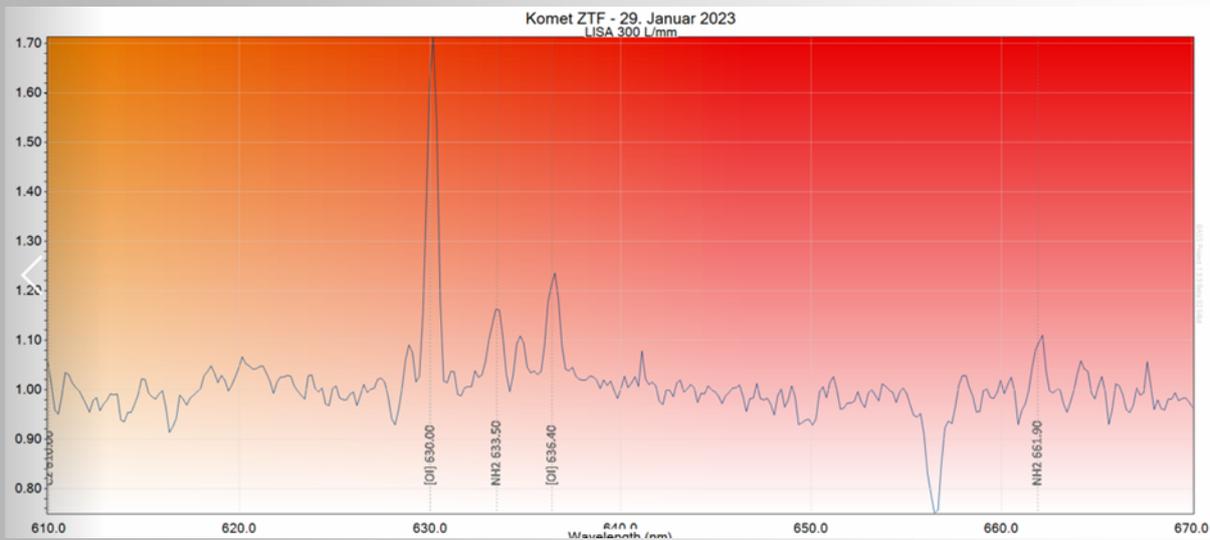
Fig. 7: Comet ZTF_29012023 with C3 molecules are also detected in comets

Despite these specialties in the spectrum, one must not forget that the main constituent of comets, and thus of C/2022 E3, if one disregards dust, is ice. This ice consists mainly of H_2O, followed by CO and CO_2, as well as frozen methane CH_4 and ammonia NH_3. When a comet approaches the sun, more and more the radiation pressure of the sun acts on the comet. The solar wind acts on the one hand mechanically (pressure) and via its charged particles also electrically (charge exchange wind/coma) and chemically (molecules).

The ice sublimates and the coma of the comet appears - and as its widely visible markers also its yellowish dust tail and its bluish ion tail.

It is now considered certain that comets are very old objects. These ice crumbs were formed about 5 billion years ago, with the formation of our solar system, that is, before the protostar progenitor of the Sun formed and well before hydrogen fusion ignited in the young Sun. Thus, the material we detect with our spectrographs in the light of the comets can rightly be called "pre-solar".